




## RESEARCH ARTICLE

# Axonal supercharged interpositional jump-graft with a hybrid artificial nerve conduit containing adipose-derived stem cells in facial nerve palsy rat model

Wataru Kamei MD<sup>1</sup>  | Hajime Matsumine MD, PhD<sup>1</sup>  | Hironobu Osaki MD, PhD<sup>2</sup> | Yoshifumi Ueta PhD<sup>2</sup> | Satoshi Tsunoda PhD<sup>1</sup> | Mari Shimizu MD<sup>1</sup> | Kazuki Hashimoto MD<sup>1</sup> | Yosuke Niimi MD, PhD<sup>1</sup>  | Mariko Miyata MD, PhD<sup>2</sup> | Hiroyuki Sakurai MD, PhD<sup>1</sup>

<sup>1</sup>Department of Plastic and Reconstructive Surgery, Tokyo Women's Medical University, Tokyo, Japan

<sup>2</sup>Department of Physiology, Division of Neurophysiology, Tokyo Women's Medical University, Tokyo, Japan

## Correspondence

Hajime Matsumine, MD, PhD, Department of Plastic and Reconstructive Surgery, Tokyo Women's Medical University, 8-1 Kawada-cho, Shinjuku-ku, Tokyo 162-8666, Japan.  
Email: matsumine@diary.ocn.ne.jp

## Funding information

This study was supported by JSPS KAKENHI, Grant/Award Number: JP16K11382; the Hiroto Yoshioka Memorial Foundation for Medical Research, the Japan-Bangladesh Medical Association Foundation, the Toho Women's Clinic Research Foundation, the Terumo Foundation for Life Sciences and Arts, and Komei Nakayama Research scholarships

**Purpose:** Interpositional jump-graft (IPJG) technique with the hypoglossal nerve for supercharging can be applied in a facial nerve palsy case. In IPJG, an autologous nerve is required, and the donor site morbidity is unavoidable. Biodegradable nerve conduits are made from polyglycolic acid (PGA) and used recently without donor site complications after providing autologous grafts. Hybrid artificial nerve conduits with adipose-derived stem cells (ASCs) also attract attention as a nerve-regeneration enhancing agent. This study examined the effect of hybrid artificial nerve conduit on IPJG.

**Materials and methods:** A total of 34 Lewis rats were used and divided into 4 groups by the bridge materials: autograft ( $n = 8$ ), PGA nerve conduit ( $n = 8$ ), hybrid PGA nerve conduit with ASCs ( $n = 8$ ), and the nontreated control groups ( $n = 8$ ). ASCs were collected from 2 rats and cultured. The animals were assessed physiologically and histopathologically at 13 weeks after surgery.

**Results:** In compound muscle action potential, the amplitude of hybrid PGA group ( $3,222 \pm 1,779 \mu\text{V}$ ) was significantly higher than that of PGA group ( $1,961 \pm 445 \mu\text{V}$ ,  $P < .05$ ), and no significant difference between hybrid PGA and autograft group. All treated groups showed a myelinated nerve regeneration with double innervation in hypoglossal and facial nerve nuclei for vibrissal muscle.

**Conclusion:** This study showed the effectiveness of IPJG with a hybrid PGA conduit especially in physiological examination.

## 1 | INTRODUCTION

Facial nerve palsy including Bell's palsy and Ramsey-Hunt syndrome appears suddenly in healthy individuals. Although remission is often focused by conservative treatment (Campbell, Hickey, Nixon, & Richardson, 1962), in some cases, persists palsy adversely reduced the quality of life. In these cases, the pathological mechanism involves the attenuation of central-nervous-system motor-nerve signals rather than organic damage to the facial nerves or mimetic muscles. A surgical treatment for these neuropathies is reported by May, Sobol, and Mester (1991). Applying an end-to-side neurorrhaphy to the facial

nerve for compensating signal attenuation with the hypoglossal nerve, they use an interpositional jump-graft (IPJG). Subsequently, many studies propose various modifications to the methodology with favorable outcomes (Ueda et al., 2007; Yamamoto et al., 2007; Yoleri, Songur, Yoleri, Vural, & Cagdas, 2000). End-to-side neurorrhaphy is studied by grafting the sciatic nerves to the fibular (Viterbo, Trindade, Hoshino, & Mazzoni Neto, 1992), sciatic (Lundborg, Zhao, Kanje, Danielsen, & Kerns, 1994), and median nerves (Hayashi et al., 2004) in the nerve defects of rat models. For treating the facial nerve palsy of rat model, (1) a cross-facial nerve graft method with sciatic nerve from the healthy to the paretic side of the face (Matsuda et al., 2008)

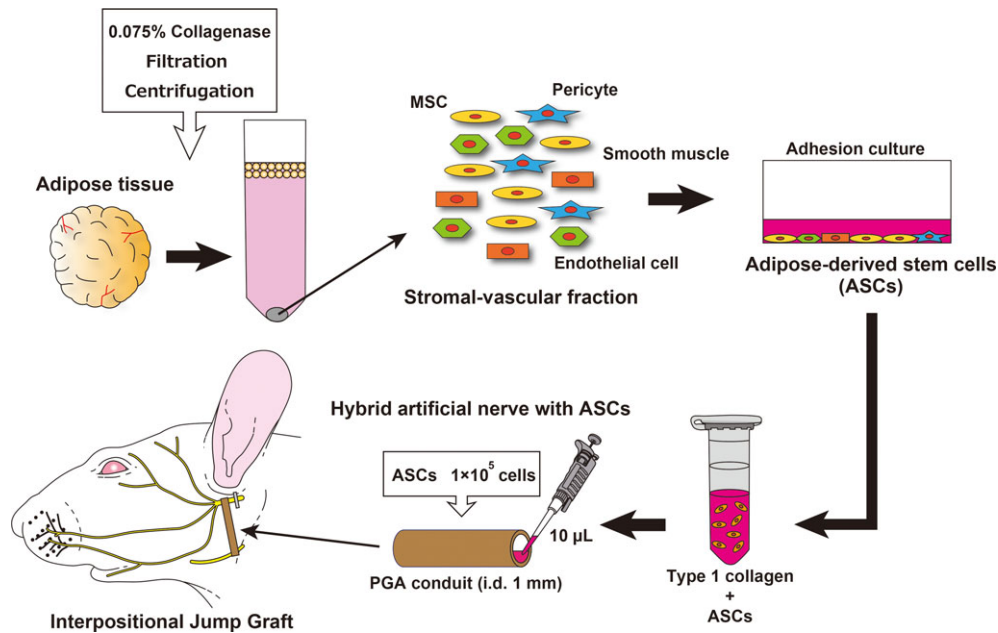


**FIGURE 1** Schematic illustration of the experimental procedures in this study. MSC indicates mesenchymal stem cell; ASCs, adipose-derived stem cells; PGA, polyglycolic acid

and (2) an end-to-side loop graft method, which harvests the buccal facial nerve branch on the healthy side and sutures the grafting nerve with nerves for creating one nerve running from the facial nerve trunk to individual branch of the facial nerve and the hypoglossal nerve (Matsumine et al., 2014), are reported. These basic studies find the functional recovery of motor nerves and axonal regeneration at the neurorrhaphy site after end-to-side neurorrhaphy. Neurorrhaphy is used with favorable outcomes in clinical settings. End-to-side sutures are used successfully from the axillary and musculocutaneous nerves to the ulnar nerve in brachial plexus palsy (Haninec, Mencl, & Kaiser, 2013). Facial nerve branches are reconstructed after the resection of various tumors with favorable outcomes, and the first report shows the effectiveness of loop grafts to the peripheral ends of facial nerve stumps with the sural nerve in a parotid tumor case (Kakibuchi et al., 2004). However, the donor site morbidity is unavoidable in cases where the auricular, sural, or other nerves is taken for autologous nerve grafts. Therefore, the authors previously investigate IPJG with silicone tubes in a rat model with facial paresis and demonstrate that the efficacy of IPJG as an artificial nerve conduit (Niimi et al., 2015). However, the recovery of facial nerve paresis treated by IPJG with the nerve conduit is found to be far inferior to that of autologous nerve grafting.

On the other hand, cellular sources for inducing nerve regeneration are speculated to be stromal vascular fraction (Matsumine et al., 2016), dedifferentiated fat cells (Matsumine et al., 2014), basic fibroblast growth factor (Matsumine et al., 2014), bone marrow stromal cells (Dezawa, Takahashi, Esaki, Takano, & Sawada, 2001), dental pulp (Sasaki et al., 2014), and adipose-derived stem cells (ASCs; Watanabe, Sasaki, Matsumine, Yamato, & Okano, 2014). Cells from these sources are used to promote peripheral nerve regeneration and especially, used in combination with artificial nerve conduits in research for exploring hybrid artificial nerve conduit approaches (Hu et al., 2017). Harvesting ASCs is performed with a minimum

invasiveness compared with other sources, and the harvested amount of the cells is easily increased. Therefore, ASCs are believed to be a potentially and clinically applicable cell source. Favorable outcomes are reported on ASC clinical applications for treating Crohn's fistula (Garcia-Olmo et al., 2005), graft-versus-host disease (Fang et al., 2007), and stress urinary incontinence (Yamamoto et al., 2012), and for cosmetic breast alteration surgery (Yoshimura et al., 2008).

For obtaining IPJGs, of which functions are closely resembles those of autologous nerve grafts, this study constructed a hybrid artificial nerve conduit with ASCs as an IPJG and evaluated the effectiveness of ASCs in the conduits for end-to-side neurorrhaphy histopathologically and physiologically.

## 2 | MATERIALS AND METHODS

All animal care and handling procedures were performed in accordance with the Principles of Laboratory Animal Care of Tokyo Women's Medical University Animal Experimentation Committee. Thirty-four male syngeneic Lewis rats were obtained from Charles River Laboratories Japan (Tokyo, Japan) and used through this study.

### 2.1 | Preparation of ASCs and hybrid polyglycolic acid-based tube

Two-eight-week-old male rats were used. Adipose tissue was collected from the inguinal region of the animal and washed with phosphate-buffered saline (PBS; Thermo Fisher Scientific, Carlsbad, CA). Cells were then isolated mechanically from the tissue and treated with 0.075% collagenase type I (Thermo Fisher Scientific) at 37 °C for 30 min, filtered through 70-µm cell strainers (BD Falcon, Becton Dickinson, Oxford, UK), neutralized by adding Dulbecco's minimum

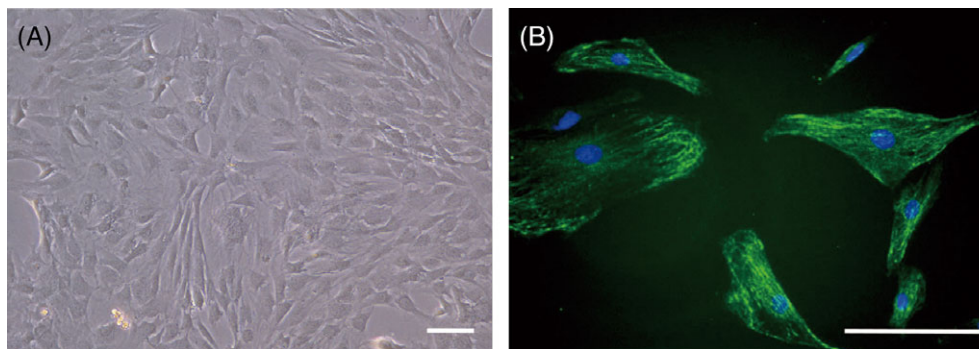


**FIGURE 2** Microphotographs of adipose-derived stem cells (ASCs) taken from adipose tissue. A, Phase-contrast microphotograph showed that ASCs had a self-propagating ability with a flattened fibroblast morphology at passage number two (P2). B, After being stained with mouse monoclonal anti-Stro-1 antibody (MAB1038; R&D systems, Minneapolis, MN), a mesenchymal stem cell (MSC) marker, and the secondary antibody, Alexa fluor 488 conjugated goat anti-mouse IgG (R37120; Thermo Fisher Scientific, Carlsbad, CA), ASCs were observed with a fluorescence microscope. In the microphotograph, the green and blue fluorescence indicate ASCs and their nuclei stained with Hoechst 33342 (H3570; Thermo Fisher Scientific), respectively. Scale bars indicate 100  $\mu\text{m}$

essential medium (Thermo Fisher Scientific) containing 10% fetal bovine serum, and centrifuged at  $800 \times g$  for 5 min. Precipitated stromal cells were re-cultured in a 100-mm tissue culture dish at  $37^\circ\text{C}$  in 5%  $\text{CO}_2$ . At 24 hr after the initiation of culture, nonadherent supernatant was removed, and the medium was exchanged with fresh medium. Cells were cultured adherently for 1 to 2 weeks at  $37^\circ\text{C}$  in 5%  $\text{CO}_2$  with medium change every 72 hr. After reaching to approximately 80% confluence, cells were detached enzymatically with 0.25% trypsin solution and passaged in fresh medium. A total of  $1 \times 10^6$  (Ueda et al., 2007) cultured cells were obtained at passage number two (P2) and put into a polyglycolic acid (PGA) tube (Nerbridge; Toyobo, Osaka, Japan) with 10  $\mu\text{L}$  type 1 collagen solution (Figure 1).

## 2.2 | ASCs as mesenchymal stem cells

ASCs showed a self-propagation ability with a flattened fibroblast morphology at P2 (Figure 2A) and were labeled with mouse monoclonal anti-Stro-1 antibody (MAB1038; R&D Systems, Minneapolis, MN), a mesenchymal stem cell marker (Figure 2B).

## 2.3 | Experimental design

The rats were divided into 4 groups. The rats belonging to the auto-graft group ( $n = 8$ ), the PGA group ( $n = 8$ ), and the hybrid PGA group ( $n = 8$ ) underwent IPJG with an ipsilateral great auricular nerve, PGA tube, and PGA tube containing ASCs, respectively, and the non-treatment rats became the control group ( $n = 8$ ). Histopathological and physiological assessments were performed at 13 weeks postoperatively.

## 2.4 | Surgical procedure

Rats were anesthetized with 3% isoflurane with an inhalation anesthesia apparatus (KN-1071 NARCOBIT-E; Natsume Seisakusho, Tokyo). After the rat was kept in a right lateral recumbent position, an S-shaped incision was made extending from behind the left ear to the

lower margin of the ipsilateral mandible (Figure 3A). The great auricular nerve was identified on the sternocleidomastoid muscle approximately 10 mm ventral to the posterior auricular surface. Dissection was advanced above the sternocleidomastoid muscle, and the facial nerve trunk was identified emerging from the anterior margin of the sternocleidomastoid muscle. The external jugular vein was then ligatured and transected, and the digastricus was identified. Dissection was advanced deeply into the digastricus, and the hypoglossal nerve was identified (Figure 3B). For preparing a rat facial nerve paresis model as reported by Shichinohe et al. (2012), a ligature clip (LIGACLIP MCA, Ethicon, OH) was allowed to crush the facial nerve trunk (Figure 3C). Subsequently, the procedures were completed for all groups. A 7-mm section was harvested from the ipsilateral great auricular nerve and used as IPJG to make the auto-graft group (Figure 3D). A 10-mm PGA tube was used as IPJG to make PGA group (Figure 3E). A 10-mm hybrid PGA tube containing ASCs was used as IPJG to make hybrid PGA group (Figure 3F). A 1.5-mm slit was made at both ends of artificial nerve conduit for inserting hypoglossal and facial nerves into the slits individually in PGA and hybrid PGA groups, and a 7-mm nerve bridge was expected to appear in the conduit. End-to-side neuroorrhaphy was performed with an epineural window on the facial or hypoglossal nerve. As the control group, rats were underwent no further treatment after the facial nerve trunk was crushed with a ligature clip. Surgery was performed with a microscope (M60; Leica Microsystems, Wetzlar, Germany).

## 2.5 | Compound muscle action potential measurement with vibrissal muscles

For assessing the functions of regenerated nerves, compound muscle action potential (CMAP) was measured. The depth of anesthesia was confirmed by observing the disappearance of eyelid reflex and the absence of whisker movement. CMAP was measured at 2 sites per rat, and the mean value was obtained from 10 successive stimulation pulses. Amplitude, duration, and latency were measured, and these

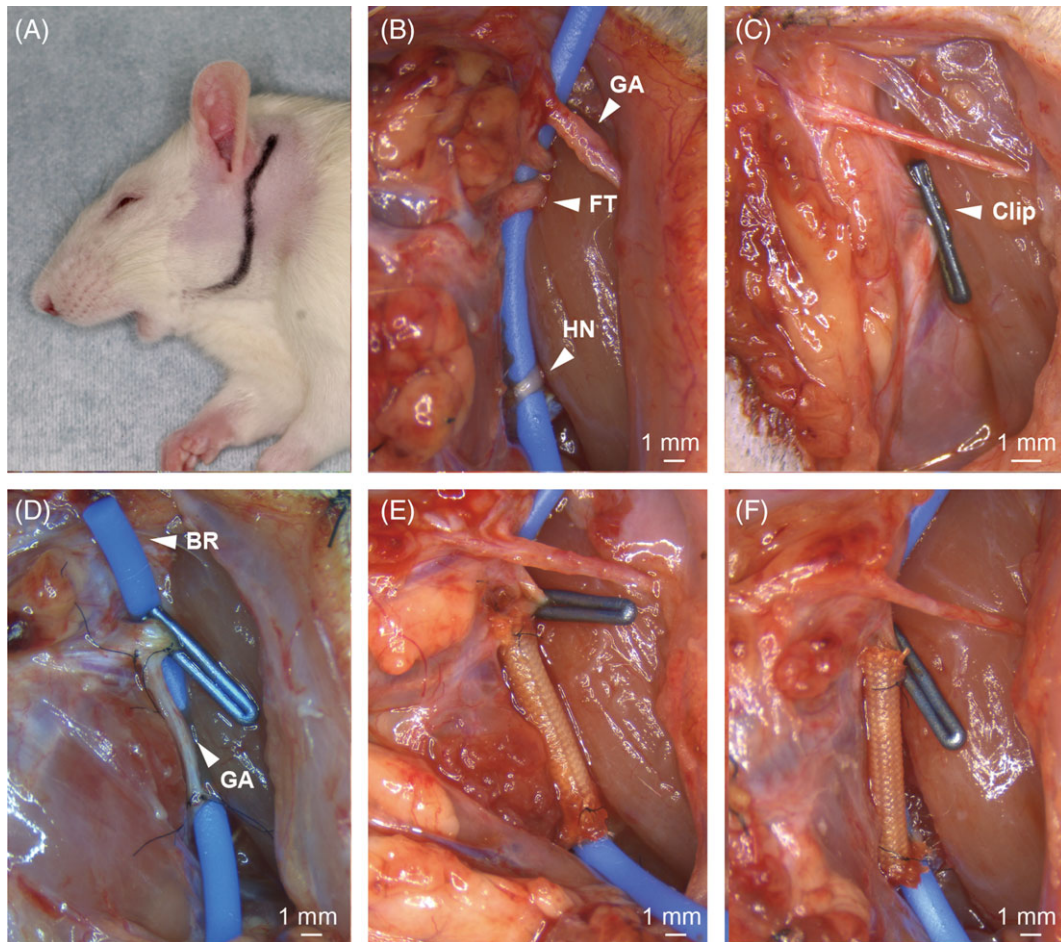


**FIGURE 3** Surgical procedures for preparing nerve palsy model. A, S-shaped incision from behind the left ear to the lower margin of the ipsilateral mandible was made. B, Facial nerve (main trunk; MT), hypoglossal nerve (HN), and greater auricular nerve (GA) were fixed. The nerves were easily recognized by a blue rubber stick (BR) placed under the nerves. C, Palsy was made by a ligature clip on the facial nerve MT. D, Interpositional jump-graft (IPJG) was performed with the ipsilateral greater auricular nerve. E, IPJG was performed with a polyglycolic acid (PGA) nerve conduit. F, IPJG was performed with a hybrid PGA nerve conduit

parameters were measured with custom-made MATLAB software (MathWorks, Natick, MA).

## 2.6 | Retrograde fluorescence tracing of facial and hypoglossal motor nuclei

Retrograde fluorescence tracers Dil (D-28) and DiO (D-275; Invitrogen, Carlsbad, CA) were injected into the left whisker pads and tongue of rats at 11 weeks postoperatively to evaluate double innervation. Rats were anesthetized with 4% isoflurane via the inhalation apparatus and injected with 100  $\mu$ L 1% Dil in ethanol and 200  $\mu$ L 0.5% DiO in N,N-dimethylformamide with a 25- $\mu$ L Hamilton syringe (Hamilton, Reno, NV). Two weeks later, rats were euthanized under deep anesthesia, and whole animal perfusion fixation was performed. The thorax and abdomen were incised, and 150 mL of 0.1 mol/L PBS was injected into the left ventricle, followed by 300 mL of 4% paraformaldehyde. The brain was extirpated and fixed with 4% paraformaldehyde and 0.2% picric acid for at least 1 day. Subsequently, 50- $\mu$ m-thick coronal sections were prepared from the brain stem with a vibratome (VT1000S; Leica Microsystems, Buffalo Grove, IL). For preparing specimens, sections were treated with 0.005% 4'6-diamidino-2-phenylindole (DAPI)

solution in the dark for 5 min and washed again with 0.1 mol/L PBS, mounted on gelatin-coated glass slides, and cover-slipped with aqueous mounting medium. Sections were then examined with a cooled charged-coupled device (CCD) camera (Quantum Scientific Imaging, Poplarville, MS) for observing Dil, DiO, and DAPI fluorescence signals.

## 2.7 | Toluidine blue staining of regenerated nerves

After CMAP measurement, the central part of the nerve graft was harvested and fixed serially with 2% paraformaldehyde, 2% glutaraldehyde, and then overnight in 0.1 mol/L cacodylate buffer solution at pH 7.4 at 4  $^{\circ}$ C. Nerve specimens were washed, postfixed with 2% osmium tetroxide, then dehydrated with ethanol, which was replaced with propylene oxide, embedded in resin (Quetol-812; Nissin EM, Tokyo). The specimen-embedded resin was allowed to polymerize for 48 hr at 60  $^{\circ}$ C. After complete polymerization, 1.5- $\mu$ m sections were prepared from the resin with an ultramicrotome (Ultracut UCT; Leica, Vienna, Austria) and stained with toluidine blue. The sliced specimens were photographed with a microscope (Leica DM ILLED; Leica). Regenerated nerves found in photographs were counted by Photoshop CC 2017 (Adobe Systems, San Jose, CA).

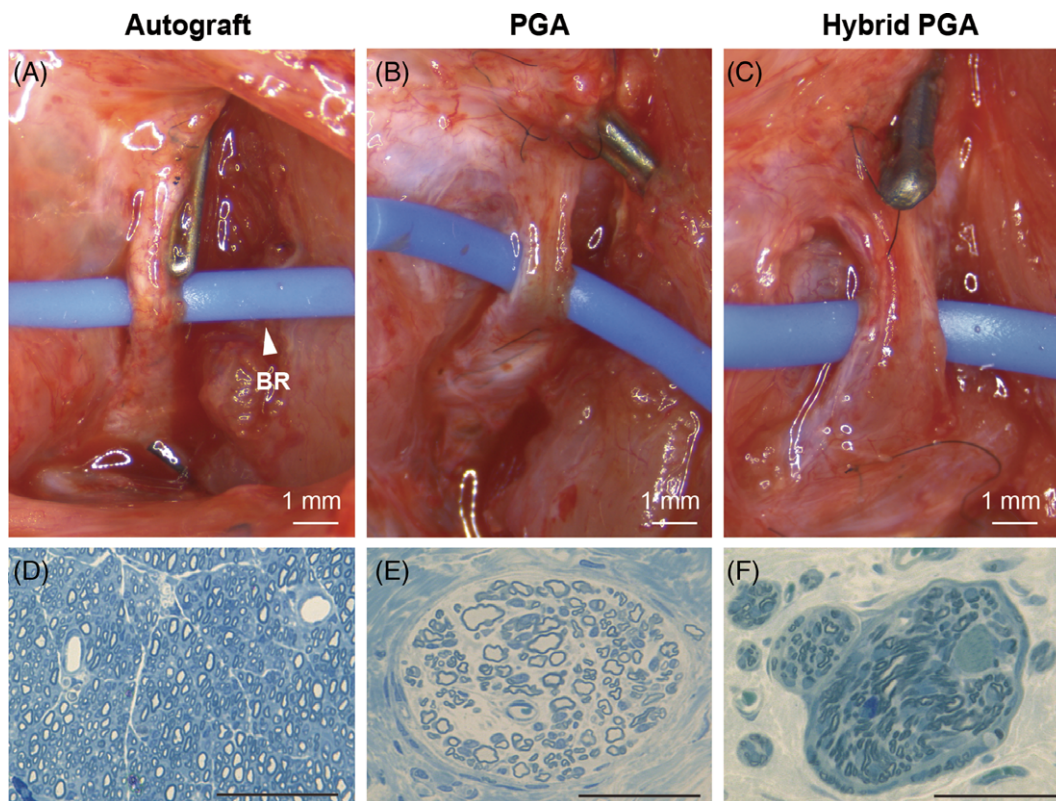


**FIGURE 4** Macroscopic findings at 13 weeks postoperatively and microphotographs of autografted nerve and nerves regenerated in nerve conduits. A, Autografted nerve was transplanted by interpositional jump-graft (IPJG) technique. B, After polyglycolic acid (PGA) nerve conduit, which was transplanted by IPJG technique, was allowed to biodegrade, regenerated nerve was exposed. C, Regenerated nerve was exposed after its PGA nerve conduit with adipose-derived stem cells (ASCs) was allowed to biodegrade. In photographs A–C, the nerves were easily recognized by blue rubber sticks (BR) placed under nerves. Microphotographs D, E, and F show the cutting sections of the central parts of autografted nerve A, and regenerated nerves B and C, respectively. The cross section specimens were stained with toluidine blue. The scale bars in the microphotographs indicate 50  $\mu\text{m}$

## 2.8 | Electron microscopic examination of regenerated nerves

Ultrathin sections with a thickness of 70 nm were prepared from resin-embedded specimens with the ultramicrotome with a diamond knife. Sections were stained with 2% uranyl acetate for 15 min at room temperature, washed with distilled water, and stained with lead stain solution (Sigma–Aldrich, St. Louis, MO) for 3 min. A JEM-1400Plus electron microscope (JEOL, Tokyo) was used at an acceleration voltage of 80 kV. Digital images were taken with a CCD camera (EM-14830RUBY2; JEOL). Fiber diameter, axon diameter, and myelin thickness were measured at 5 randomly selected sites by Photoshop CC 2017.

## 2.9 | Statistical analysis

Mean values and standard deviations were calculated for data obtained from CMAP measurements, toluidine blue staining, and electron microscopy. *P* values less than .05 ( $P < .05$ ) were considered significant. Data from individual groups were analyzed with analysis of variance (ANOVA) and Tukey's multiple comparison test, using JMP<sup>®</sup> software, version 13 (SAS Institute, Cary, NC).

## 3 | RESULTS

All rats survived after surgery, and no animal showed any complications. Autograft, PGA, and hybrid PGA groups showed macroscopic nerve regeneration at 13 weeks postoperatively (Figure 4A–C). Toluidine blue stained specimens revealed myelin sheath and axonal regeneration in autograft (Figure 4D), PGA (Figure 4E), and hybrid PGA groups (Figure 4F). Distinct dense nerve regeneration was observed in the autograft group compared with PGA and hybrid PGA groups. Electron microscopy revealed myelinated nerve regeneration in the autograft (Figure 5A), PGA (Figure 5B), and hybrid PGA groups (Figure 5C). Mean number of regenerated myelinated fibers of autograft group ( $1,852 \pm 365$ ) was significantly higher than those of other 2 IPJG treatment groups ( $P < .01$ ); hybrid PGA group ( $320 \pm 210$ ) and PGA group ( $177 \pm 78$ ; Figure 6A).

Mean nerve fiber diameter of autograft group ( $5.7 \pm 2.2 \mu\text{m}$ ; Figure 6B) was significantly higher than those of PGA ( $4.5 \pm 0.2 \mu\text{m}$ ;  $P < .01$ ) and hybrid PGA groups ( $5.0 \pm 2.2 \mu\text{m}$ ;  $P < .05$ ).

No significant differences in axon diameter (Figure 6C) were found among autograft ( $4.2 \pm 1.8 \mu\text{m}$ ), PGA ( $3.6 \pm 2.0 \mu\text{m}$ ), and hybrid PGA groups ( $3.6 \pm 1.9 \mu\text{m}$ ).

Myelin thickness of autograft group ( $0.79 \pm 0.03 \mu\text{m}$ ) was significantly higher than that of hybrid PGA group ( $0.68 \pm 0.29 \mu\text{m}$ ;

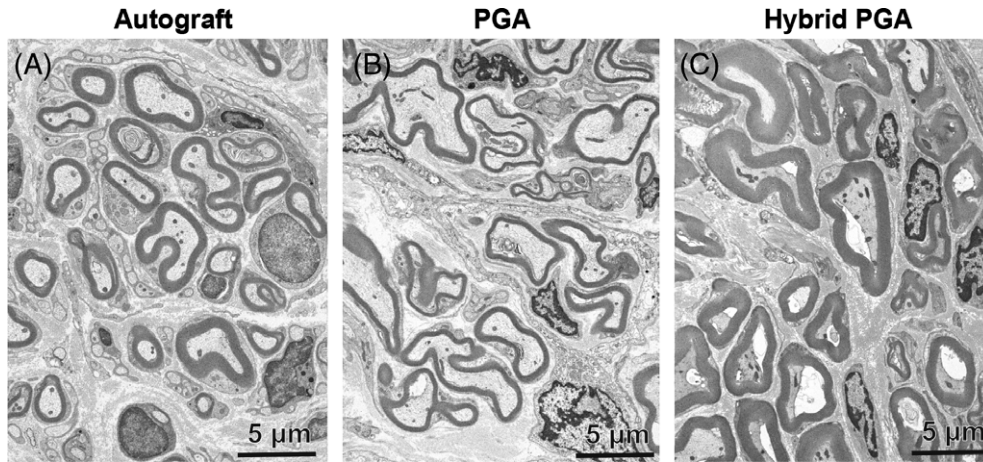


**FIGURE 5** Electron microphotographs of the cross sections of autografted and regenerated nerves at 13 weeks after surgery. Electron microphotographs A-C show the cross sections of the central parts of autografted nerve, and regenerated nerves in polyglycolic acid (PGA) nerve conduit and hybrid PGA conduit with adipose-derived stem cells (ASCs), respectively. In the photographs, myelinated cells were observed to regenerate. The scale bars indicate 5  $\mu\text{m}$

$P < .01$ ), and that of hybrid PGA group was significantly higher than that of PGA group ( $0.44 \pm 0.03 \mu\text{m}$ ;  $P < .01$ ; Figure 6D).

The  $g$  ratio (axon/fiber diameter ratio) of PGA group ( $0.80 \pm 0.15$ ;  $P < .01$ ) was significantly higher than those of autograft and hybrid PGA groups (Figure 6E).

CMAP measurement revealed muscle contractions after stimulation in all groups (Figure 7A-D). Amplitude was greatest in autograft group ( $4,352 \pm 1,587 \mu\text{V}$ ), followed by hybrid PGA ( $3,222 \pm 1,779 \mu\text{V}$ ), PGA

( $1,961 \pm 445 \mu\text{V}$ ), and the control groups ( $687 \pm 490 \mu\text{V}$ ; Figure 7E). The amplitude of hybrid PGA group was found to be significantly higher than that of PGA group. Duration of PGA group ( $0.49 \pm 0.14 \text{ ms}$ ) was shortest among other groups; hybrid PGA ( $0.52 \pm 0.14 \text{ ms}$ ), autograft ( $0.95 \pm 0.68 \text{ ms}$ ), and the control groups ( $1.11 \pm 0.53 \text{ ms}$ ; Figure 7F). Duration values of PGA and hybrid PGA groups were significantly shorter than those of the control and autograft groups ( $P < .05$ ). Latency was shortest in the autograft group ( $2.8 \pm 0.9 \text{ ms}$ ), followed by hybrid

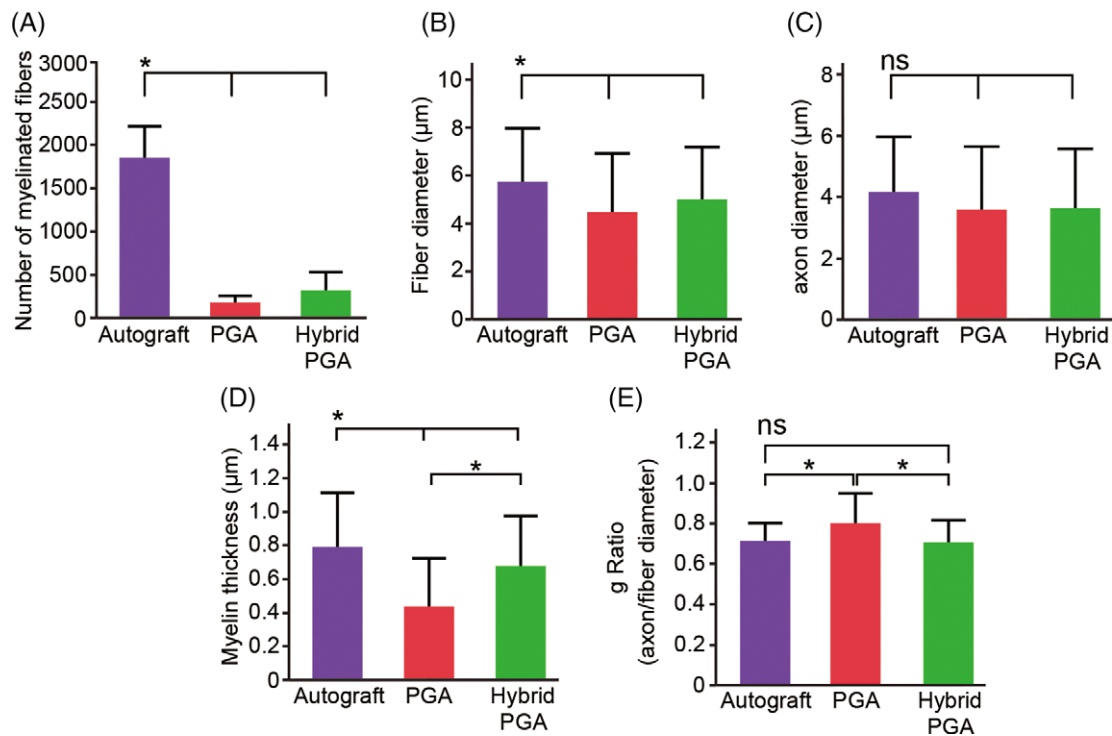


**FIGURE 6** Number of myelinated fibers, fiber diameter, and axon diameter, myelin thickness, and axon/fiber diameter ratio ( $g$  ratio) of autograft, PGA, and hybrid PGA groups. A, The number of regenerated myelinated fibers; B, the regenerated fiber diameter; C, the axon diameter; D, the myelin thickness; E,  $g$  ratio, which was calculated by dividing axon with fiber diameters, of autograft nerve, and regenerated nerves in polyglycolic acid (PGA) nerve conduit and hybrid PGA conduit with adipose-derived stem cells (ASCs) are shown. One asterisk (\*) indicates a probability of less than .05, and "ns" indicates nonsignificant

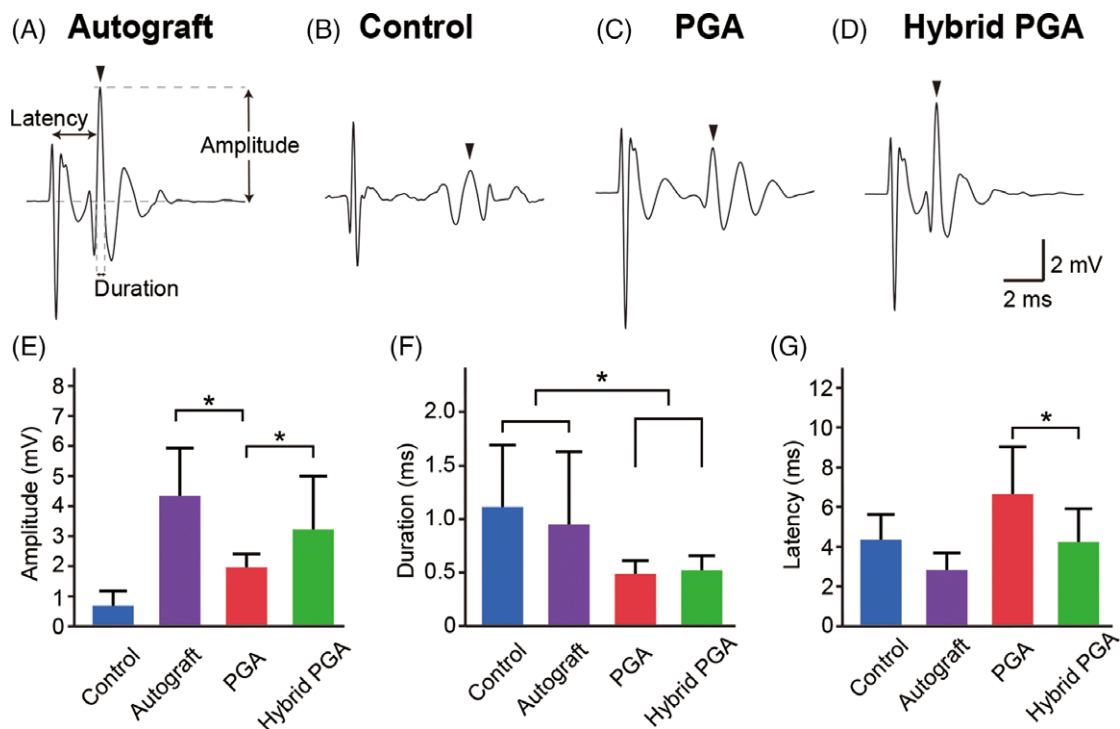


**FIGURE 7** Results of compound muscle action potential (CMAP) analysis. In the upper row, CMAP wave patterns A, B, C, and D were taken from rats of autograft, the control (nontreated), polyglycolic acid (PGA), and hybrid PGA groups, respectively. In the lower row, bar graphs E, F, and G show the amplitude, the duration, and the latency data of autograft, the control (nontreated), PGA, and hybrid PGA groups, respectively. One asterisk (\*) indicates a probability of less than .05, and “ns” indicates nonsignificant

PGA ( $4.3 \pm 1.7$  ms), the control ( $4.4 \pm 0.4$  ms), and PGA group ( $6.6 \pm 2.8$  ms; Figure 7G). Latency was significantly shorter in hybrid PGA than PGA groups ( $P < .01$ ).

Retrograde tracer examinations revealed Dil and DiO-positive motor neurons in both facial nerve nuclei (7N) and hypoglossal nuclei (12N) in the control group (Figure 8A,B). On the other hand, autograft, PGA, and hybrid PGA groups, Dil and DiO-positive motor neurons were observed in both 7N and 12N with double innervation (Figure 8C-J), indicating that the double innervation of mimetic muscles in 7N and 12N.

## 4 | DISCUSSION

Although the histopathological results of this study showed that the number of myelinated fibers of hybrid PGA group was unable to reach to that of autograft group, and the regenerated axonal thickness of hybrid PGA was comparable to that of autograft group, and the thickness of the myelin sheath was thicker than that of PGA group. The physiological results by CMAP showed that hybrid PGA-treated rats showed a significantly greater amplitude value than PGA-treated rats, and the amplitude value was comparable to that of autograft rats. These results demonstrated that ASCs in conduits promoted nerve regeneration and thicker myelin-sheath formation after nerve conduits bridged nerves by end-to-side neurorrhaphy. Although the number of regenerated myelinated fibers of the hybrid PGA group was lower than that of the autograft group, in the *g*-ratio representing the axonal myelination (Chomiak & Hu, 2009), there was no significant difference between these 2 groups, indicating that the quality of the

regenerated nerve of the hybrid PGA group was comparable to that of the autograft group.

The retrograde results proved that end-to-side neurorrhaphy allowed regenerated nerves to have double innervation by functional facial and hypoglossal nerve neurons. Previously, experiments on retrograde tracers from whisker pads and tongues are performed in a model similar to that of this study for investigating interactive nerve regeneration (Niimi et al., 2015; Niimi et al., 2018). Referring the results of the references, the authors speculated that this study's model also proved no facial complete paralysis, indicating that IPJG provided double innervation to the mimetic muscles.

Previously, hybrid artificial nerve conduits containing ASCs are investigated in rats with sciatic nerve deficit (Erba et al., 2010). Although ASCs are unable to survive through 2 weeks after transplantation, they are considered to promote nerve regeneration by secreting neurotrophic factors such as nerve growth factor (NGF; Peeraully, Jenkins, & Trayhurn, 2004), brain-derived neurotrophic factor (BDNF; Wei et al., 2009) and vascular endothelial growth factor (Sondell, Lundborg, & Kanje, 1999) in the early posttransplant period. ASCs reportedly transform into Schwann-like cells with exudate released from damaged sciatic nerve in rats (Liu et al., 2013), and the transformation was considered to be performed by secreted NGF, BDNF, and neurotrophin 3 from healthy Schwann cells in the deficient nerve. Therefore, the mechanism of ASC-promoted nerve regeneration in this study might consist of 2 serial paracrine actions: (1) the release of neurotrophic factors from the grafted ASCs in artificial nerve conduit and (2) the transformation of ASCs into Schwann-like cells with released neurotrophic factors from facial and hypoglossal nerves at

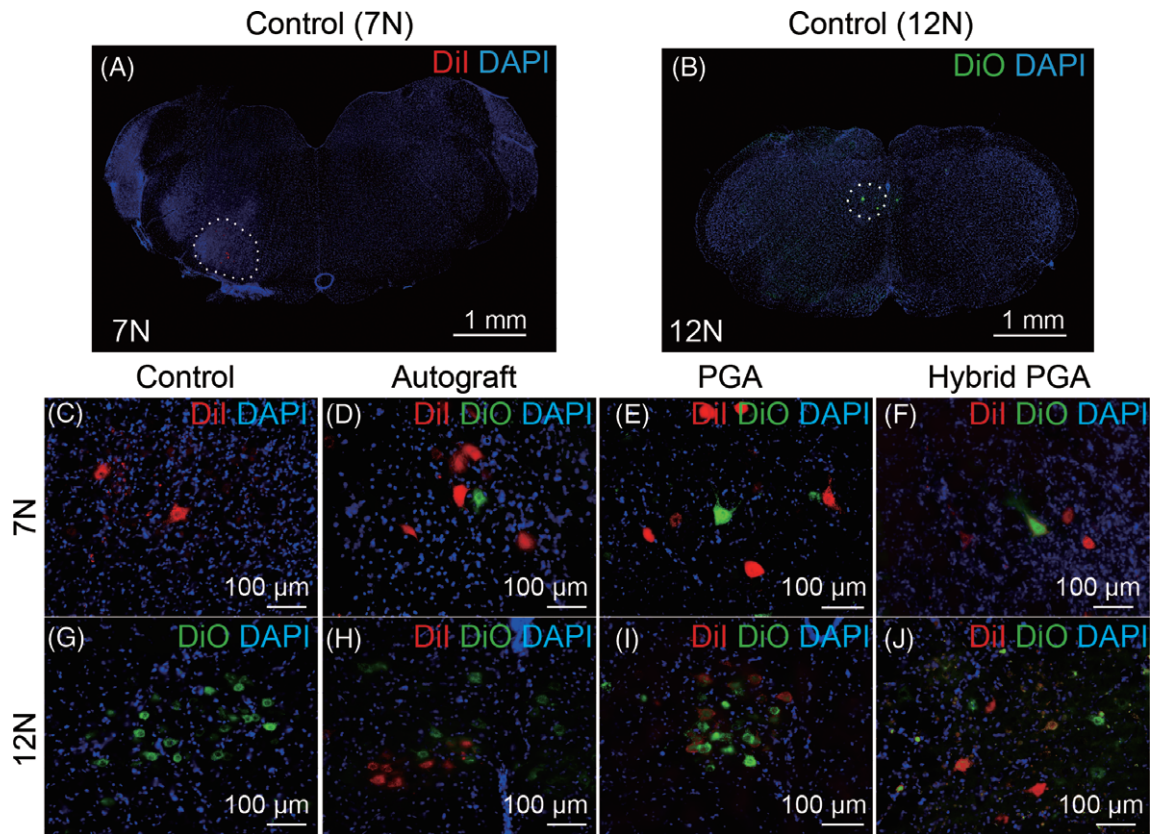


**FIGURE 8** Results of retrograde fluorescence tracing at 13 weeks postoperatively. In the upper row, the white-dot-circles in photographs A and B show facial (7N) and hypoglossal nerve nuclei (12N), respectively. The middle and lower rows show the facial nerve nucleus (7N) and the hypoglossal nerve nucleus (12N), respectively. The first, second, third, and fourth columns show the specimens of the control, autograft, polyglycolic acid (PGA), and hybrid PGA groups, respectively. In photograph C, 7N of the control was marked with Dil-positive (red) motor neuron, and in photograph G, 12N of the control was marked with DiO-positive (green) motor neuron. In photographs from D to F and H to J, double innervation was confirmed by observing both 7N and 12N in autograft, PGA, and hybrid PGA groups

the host sites where epineural windows were made by end-to-side neurorrhaphy.

These experimental models were incomplete paralysis models and suitable for investigating the efficacy of neural supercharging from the hypoglossal nerve to the facial nerve, because IPJG procedure is a technique for an incomplete facial paralysis in clinical cases. Classical IPJG technique contains the axotomy of the hypoglossal nerve. However, the subsequent development of basic research on end-to-side neurorrhaphy highlights new techniques such as the fenestrations of the epineurium and the perineurium, and end-to-side neurorrhaphy without the host-site axotomy. Nerve fiber influx is observed in the regenerated nerves treated by these techniques (Matsumoto et al., 1999; Viterbo, Trindade, Hoshino, & Mazzoni, 1994). Axotomy is reported to promote collateral spouting (Hayashi et al., 2008). In this study, epineural windows were made by a technique similar to IPJG method reported by Ueda et al. (2007), because the technique could avoid damaging the functions of the residual facial nerves, or the hypoglossal nerve, which are known to be the source of supercharging. Therefore, this study performed neurorrhaphy with the technique meticulously for reducing the risk of axonal damage. Since the murine hypoglossal nerve lies deeply within the cervical region and end-to-side neurorrhaphy with a 1-mm diameter artificial conduit could be difficult, this study was able to successfully perform the procedure with untied sutures for both the hypoglossal nerve and facial

nerve sides. Further studies including an investigation on differences in nerve regeneration between axotomy and nonaxotomy groups and investigations on comorbidities such as the atrophy of the tongue were required.

This study performed a 7-mm IPJG in a rat facial nerve palsy model and obtained favorable outcomes in hybrid PGA group. However, a nerve bridge of around 50 to 70 mm in length will be required in clinical use. Currently, there is no data showing the size of nerve deficit where a hybrid conduit is effective. Future research using larger experimental animals with longer artificial nerve conduits is needed to confirm the limit of the range where regeneration can be achieved. This is the first report of end-to-side nerve neurorrhaphy with hybrid artificial nerve conduits containing ASCs. The regeneration of myelinated fibers within the central part of the graft in all treatment groups was observed, and these morphological data indicated that ASCs promoted nerve regeneration even in the artificial nerve conduits, which was used end-to-side neurorrhaphy.

## 5 | CONCLUSION

This study successfully demonstrated end-to-side neurorrhaphy for the facial and hypoglossal nerves with a hybrid PGA nerve conduit containing ASCs, which promote nerve regeneration for the



neurorrhaphy. This study clarified that the technique could potentially come closer to conventional IPJG techniques with autologous grafts.

## ACKNOWLEDGMENTS

This study was supported by Japan Society for the Promotion of Science KAKENHI Grant Number JP16K11382, the Hiroto Yoshioka Memorial Foundation for Medical Research, the Japan–Bangladesh Medical Association Foundation, the Toho Women's Clinic Research Foundation, the Terumo Foundation for Life Sciences and Arts, and Komei Nakayama Research scholarships.

## CONFLICT OF INTEREST

None.

## ORCID

Wataru Kamei  <https://orcid.org/0000-0001-7725-9123>

Hajime Matsumine  <https://orcid.org/0000-0001-6158-1169>

Yosuke Niimi  <https://orcid.org/0000-0002-4203-380X>

## REFERENCES

- Campbell, E. D., Hickey, R. P., Nixon, K. H., & Richardson, A. T. (1962). Value of nerve-excitability measurements in prognosis of facial palsy. *British Medical Journal*, 2(5296), 7–10.
- Chomiak, T., & Hu, B. (2009). What is the optimal value of the g-ratio for myelinated fibers in the rat CNS? A theoretical approach. *PLoS One*, 4(11), e7754.
- Dezawa, M., Takahashi, I., Esaki, M., Takano, M., & Sawada, H. (2001). Sciatic nerve regeneration in rats induced by transplantation of in vitro differentiated bone-marrow stromal cells. *The European Journal of Neuroscience*, 14(11), 1771–1776.
- Erba, P., Mantovani, C., Kalbermatten, D. F., Pierer, G., Terenghi, G., & Kingham, P. J. (2010). Regeneration potential and survival of transplanted undifferentiated adipose tissue-derived stem cells in peripheral nerve conduits. *Journal of Plastic, Reconstructive & Aesthetic Surgery*, 63(12), e811–e817.
- Fang, B., Song, Y., Lin, Q., Zhang, Y., Cao, Y., Zhao, R. C., & Ma, Y. (2007). Human adipose tissue-derived mesenchymal stromal cells as salvage therapy for treatment of severe refractory acute graft-vs.-host disease in two children. *Pediatric Transplantation*, 11(7), 814–817.
- García-Olmo, D., García-Arranz, M., Herreros, D., Pascual, I., Peiro, C., & Rodríguez-Montes, J. A. (2005). A phase I clinical trial of the treatment of Crohn's fistula by adipose mesenchymal stem cell transplantation. *Diseases of the Colon and Rectum*, 48(7), 1416–1423.
- Haninac, P., Mencl, L., & Kaiser, R. (2013). End-to-side neurorrhaphy in brachial plexus reconstruction. *Journal of Neurosurgery*, 119(3), 689–694.
- Hayashi, A., Pannucci, C., Moradzadeh, A., Kawamura, D., Magill, C., Hunter, D. A., ... Myckatyn, T. M. (2008). Axotomy or compression is required for axonal sprouting following end-to-side neurorrhaphy. *Experimental Neurology*, 211(2), 539–550.
- Hayashi, A., Yanai, A., Komuro, Y., Nishida, M., Inoue, M., & Seki, T. (2004). Collateral sprouting occurs following end-to-side neurorrhaphy. *Plastic and Reconstructive Surgery*, 114(1), 129–137.
- Hu, F., Zhang, X., Liu, H., Xu, P., Doulathunnisa, T. G., & Xiao, Z. (2017). Neuronally differentiated adipose-derived stem cells and aligned PHBV nanofiber nerve scaffolds promote sciatic nerve regeneration. *Biochemical and Biophysical Research Communications*, 489(2), 171–178.
- Kakibuchi, M., Tuji, K., Fukuda, K., Terada, T., Yamada, N., Matsuda, K., ... Sakagami, M. (2004). End-to-side nerve graft for facial nerve reconstruction. *Annals of Plastic Surgery*, 53(5), 496–500.
- Liu, Y., Zhang, Z., Qin, Y., Wu, H., Lv, Q., Chen, X., & Deng, W. (2013). A new method for Schwann-like cell differentiation of adipose derived stem cells. *Neuroscience Letters*, 551, 79–83.
- Lundborg, G., Zhao, Q., Kanje, M., Danielsen, N., & Kerns, J. M. (1994). Can sensory and motor collateral sprouting be induced from intact peripheral nerve by end-to-side anastomosis? *The Journal of Hand Surgery: British & European Volume*, 19(3), 277–282.
- Matsuda, K., Kakibuchi, M., Kubo, T., Tomita, K., Fujiwara, T., Hattori, R., ... Hosokawa, K. (2008). A new model of end-to-side nerve graft for multiple branch reconstruction: End-to-side cross-face nerve graft in rats. *Journal of Plastic, Reconstructive & Aesthetic Surgery*, 61(11), 1357–1367.
- Matsumine, H., Numakura, K., Klimov, M., Watanabe, Y., Giatsidis, G., & Orgill, D. P. (2016). Facial-nerve regeneration ability of a hybrid artificial nerve conduit containing uncultured adipose-derived stromal vascular fraction: An experimental study. *Microsurgery*, 37(7), 808–818.
- Matsumine, H., Sasaki, R., Tabata, Y., Matsui, M., Yamato, M., Okano, T., & Sakurai, H. (2014). Facial nerve regeneration using basic fibroblast growth factor-impregnated gelatin microspheres in a rat model. *Journal of Tissue Engineering and Regenerative Medicine*, 10(10), E559–E567.
- Matsumine, H., Sasaki, R., Takeuchi, Y., Watanabe, Y., Niimi, Y., Sakurai, H., ... Yamato, M. (2014). Unilateral multiple facial nerve branch reconstruction using "end-to-side loop graft" supercharged by hypoglossal nerve. *Plastic and Reconstructive Surgery—Global Open*, 2(10), e240.
- Matsumine, H., Takeuchi, Y., Sasaki, R., Kazama, T., Kano, K., Matsumoto, T., ... Yamato, M. (2014). Adipocyte-derived and dedifferentiated fat cells promoting facial nerve regeneration in a rat model. *Plastic and Reconstructive Surgery*, 134(4), 686–697.
- Matsumoto, M., Hirata, H., Nishiyama, M., Morita, A., Sasaki, H., & Uchida, A. (1999). Schwann cells can induce collateral sprouting from intact axons: Experimental study of end-to-side neurorrhaphy using a Y-chamber model. *Journal of Reconstructive Microsurgery*, 15(4), 281–286.
- May, M., Sobol, S. M., & Mester, S. J. (1991). Hypoglossal-facial nerve interpositional-jump graft for facial reanimation without tongue atrophy. *Otolaryngology and Head and Neck Surgery*, 104(6), 818–825.
- Niimi, Y., Matsumine, H., Takeuchi, Y., Osaki, H., Tsunoda, S., Miyata, M., ... Sakurai, H. (2018). A collagen-coated PGA conduit for interpositional-jump graft with end-to-side neurorrhaphy for treating facial nerve paralysis in rat. *Microsurgery* (in press).
- Niimi, Y., Matsumine, H., Takeuchi, Y., Sasaki, R., Watanabe, Y., Yamato, M., ... Sakurai, H. (2015). Effectively axonal-supercharged interpositional jump-graft with an artificial nerve conduit for rat facial nerve paralysis. *Plastic and Reconstructive Surgery—Global Open*, 3(6), e416.
- Peeraully, M. R., Jenkins, J. R., & Trayhurn, P. (2004). NGF gene expression and secretion in white adipose tissue: Regulation in 3T3-L1 adipocytes by hormones and inflammatory cytokines. *American Journal of Physiology. Endocrinology and Metabolism*, 287(2), E331–E339.
- Sasaki, R., Matsumine, H., Watanabe, Y., Takeuchi, Y., Yamato, M., Okano, T., ... Ando, T. (2014). Electrophysiologic and functional evaluations of regenerated facial nerve defects with a tube containing dental pulp cells in rats. *Plastic and Reconstructive Surgery*, 134(5), 970–978.
- Shichinohe, R., Furukawa, H., Sekido, M., Saito, A., Hayashi, T., Funayama, E., ... Yamamoto, Y. (2012). Direction of innervation after interpositional nerve graft between facial and hypoglossal nerves in individuals with or without facial palsy: A rat model for treating incomplete facial palsy. *Journal of Plastic, Reconstructive & Aesthetic Surgery*, 65(6), 763–770.
- Sondell, M., Lundborg, G., & Kanje, M. (1999). Vascular endothelial growth factor has neurotrophic activity and stimulates axonal outgrowth, enhancing cell survival and Schwann cell proliferation in the peripheral nervous system. *The Journal of Neuroscience*, 19(14), 5731–5740.
- Ueda, K., Akiyoshi, K., Suzuki, Y., Ohkouchi, M., Hirose, T., Asai, E., & Tateshita, T. (2007). Combination of hypoglossal-facial nerve jump graft by end-to-side neurorrhaphy and cross-face nerve graft for the treatment of facial paralysis. *Journal of Reconstructive Microsurgery*, 23(4), 181–187.
- Viterbo, F., Trindade, J. C., Hoshino, K., & Mazzoni, A. (1994). Two end-to-side neurorrhaphies and nerve graft with removal of the

- epineural sheath: Experimental study in rats. *British Journal of Plastic Surgery*, 47(2), 75–80.
- Viterbo, F., Trindade, J. C., Hoshino, K., & Mazzone Neto, A. (1992). Latero-terminal neurotomy without removal of the epineural sheath. Experimental study in rats. *Revista Paulista de Medicina*, 110(6), 267–275.
- Watanabe, Y., Sasaki, R., Matsumine, H., Yamato, M., & Okano, T. (2014). Undifferentiated and differentiated adipose-derived stem cells improve nerve regeneration in a rat model of facial nerve defect. *Journal of Tissue Engineering and Regenerative Medicine*, 11(2), 362–374.
- Wei, X., Du, Z., Zhao, L., Feng, D., Wei, G., He, Y., ... Du, Y. (2009). IFATS collection: The conditioned media of adipose stromal cells protect against hypoxia-ischemia-induced brain damage in neonatal rats. *Stem Cells*, 27(2), 478–488.
- Yamamoto, T., Gotoh, M., Kato, M., Majima, T., Toriyama, K., Kamei, Y., ... Funahashi, Y. (2012). Periurethral injection of autologous adipose-derived regenerative cells for the treatment of male stress urinary incontinence: Report of three initial cases. *International Journal of Urology*, 19(7), 652–659.
- Yamamoto, Y., Sekido, M., Furukawa, H., Oyama, A., Tsutsumida, A., & Sasaki, S. (2007). Surgical rehabilitation of reversible facial palsy: Facial-hypoglossal network system based on neural signal augmentation/neural supercharge concept. *Journal of Plastic, Reconstructive & Aesthetic Surgery*, 60(3), 223–231.
- Yoleri, L., Songur, E., Yoleri, O., Vural, T., & Cagdas, A. (2000). Reanimation of early facial paralysis with hypoglossal/facial end-to-side neurotomy: A new approach. *Journal of Reconstructive Microsurgery*, 16(5), 347–355 discussion 355–346.
- Yoshimura, K., Sato, K., Aoi, N., Kurita, M., Hirohi, T., & Harii, K. (2008). Cell-assisted lipotransfer for cosmetic breast augmentation: Supportive use of adipose-derived stem/stromal cells. *Aesthetic Plastic Surgery*, 32(1), 48–55 discussion 56–47.

**How to cite this article:** Kamei W, Matsumine H, Osaki H, et al. Axonal supercharged interpositional jump-graft with a hybrid artificial nerve conduit containing adipose-derived stem cells in facial nerve palsy rat model. *Microsurgery*. 2018;38: 889–898. <https://doi.org/10.1002/micr.30389>